

# Direct-UV-written buried channel waveguide lasers in direct-bonded intersubstrate ion-exchanged Nd:SGBN glass

Corin B. E. Gawith, Alexander Fu, Tajamal Bhutta, Ping Hua, David P. Shepherd, Elizabeth R. Taylor, and Peter G. R. Smith  
*Optoelectronics Research Centre, University of Southampton, SO17 1BJ, United Kingdom*

Daniel Milanese and Monica Ferraris  
*Politecnico di Torino, Corso Duca degli Abruzzi 24, 10129 Torino, Italy*

(Received...)

We report a technique for producing single-mode buried channel waveguide lasers in neodymium-doped SGBN glass. Direct bonding forms the basis of this process, providing a buried waveguide layer in the photosensitive SGBN material into which channel confinement can be directly written with a focussed UV beam. Characterization of a 7.5-mm-long device was performed using a Ti:Sapphire laser operating at 808 nm and the resultant 1059 nm channel waveguide laser output exhibited single-mode operation, milliwatt-order lasing thresholds, and propagation losses of  $< 0.3 \text{ dB cm}^{-1}$ .  
 [Letter number...]

Ion-exchange techniques provide a simple and versatile basis for creating optical planar waveguide devices in glass<sup>1</sup>. As the demand for novel telecommunications devices grows, increased emphasis has been placed on improving the host glasses for a range of functions, such as rare-earth doping for integrated optical sources and amplifiers<sup>2</sup>, and creating devices with symmetric mode profiles and low losses suitable for coupling to single mode fibers<sup>1</sup>. While such characteristics can be achieved by burying waveguides below the surface of an ion-exchanged substrate using a secondary diffusion or E-field assisted process, we have recently developed an alternative technique for producing buried planar waveguide lasers in neodymium-doped BK-7 by solid-state  $\text{K}^+ \text{-Na}^+$  ion-exchange with an adjoining potassium-rich borosilicate cladding substrate<sup>3</sup>. Direct bonding<sup>4</sup> forms the basis of this process, providing a region of atomic contact between the two glass layers and a 350 °C thermal treatment suitable for simultaneous bond strengthening and intersubstrate ion-exchange, resulting in a single-step buried ion-exchange mechanism with inherently low waveguide losses. Here, we present a refinement of this technique, as germania-doped photosensitivity is incorporated into the host substrate material to allow more complex waveguide structures to be formed by direct UV writing into the buried waveguide layer.

The direct UV writing<sup>5</sup> technique has recently received considerable scientific interest as a potential route towards low-cost integrated optical components in glass. Based on a localised change in refractive index induced by short-wave radiation, this technique allows waveguide structures to be literally drawn into a photosensitive material by computer-controlled scanning of a focussed UV beam, eliminating the development time and costs associated with repeated photolithographic steps. Used in the design and fabrication of various optical devices, ranging from channel waveguides<sup>5</sup> towards more complex structures based on Bragg gratings<sup>6</sup> and directional couplers<sup>7</sup>, the majority of direct UV writing processes to date have been performed on buried thin film

germanosilicate layers based on Plasma Enhanced Chemical Vapour Deposition (PECVD) silica-on-silicon wafers. Such multilayered structures are designed to allow UV-writing through a cladding layer and down into the photosensitive material, offering improved mode quality, low losses, and efficient coupling to optical fibers<sup>5</sup>.

Combining photosensitivity with intersubstrate ion-exchange provides a hybrid route towards creating buried channel waveguide structures in bulk glass materials (Fig. 1), which have the potential advantages of being simpler to produce and more readily tailored to incorporate large amounts of exotic and volatile components (high phosphorus content, erbium-ytterbium co-doping etc.) not usually available by wafer deposition techniques<sup>8</sup>. One such material to be recently developed is SGBN<sup>8,9</sup>, a bulk multicomponent oxide glass named after its main constituent parts of Silica, Germania, Boron, and Sodium (Na), and the first designed to incorporate simultaneous Ge-based photosensitivity, ion-exchangeability, and rare-earth doping (although never before in the same device). Previous experiments performed with SGBN have demonstrated UV-written waveguide structures through almost a millimeter of the bulk material<sup>8</sup>, providing the large penetration depth required for UV writing into a

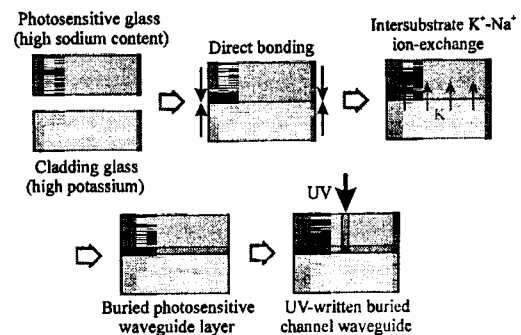


FIG. 1: Key processing stages in the design and fabrication of a buried channel waveguide laser by a combination of direct bonding and direct UV writing techniques.

buried ion-exchanged layer, although high propagation losses of several  $\text{dB cm}^{-1}$  had previously prevented laser action in the rare-earth-doped photosensitive material.

In this letter we describe the successful development of buried channel waveguide lasers in neodymium-doped SGBN glass by a combination of direct bonding and direct UV writing techniques. Based on our previously presented intersubstrate ion-exchange technique, we have used direct bonding to provide a region of atomic contact between Nd:SGBN and a potassium-rich borosilicate cladding substrate, between which  $\text{K}^+\text{-Na}^+$  ion-exchange can occur. By taking this approach we have achieved a low-loss buried planar waveguide layer in the Nd:SGBN glass, which retains the photosensitive characteristics of the bulk material and into which single-mode channel waveguide structures can be directly written using a focussed UV beam.

Fabrication of the rare-earth-doped SGBN substrate used in this experiment (illustrated as the top layer in Fig. 1) began by melting batch powders of  $\text{SiO}_2$  (60 wt.%),  $\text{GeO}_2$  (10 wt.%),  $\text{B}_2\text{O}_3$  (10 wt.%),  $\text{Na}_2\text{O}$  (19 wt.%), and  $\text{Nd}_2\text{O}_3$  (1 wt.%), in a resistance furnace for 2 hours. The SGBN glass was doped to include previously optimised concentrations of germanium for photosensitivity<sup>8</sup> and sodium for ion-exchange<sup>9</sup>, and a small (unoptimised) amount of neodymium was also added to facilitate laser action for this initial demonstration. A temperature range of 850 °C to 1450 °C was available throughout the doping process, the melt being fired at 1400 °C and removed from the furnace at 1300 °C. The glass was then cast onto a preheated copper plate and slowly returned to room temperature to promote structural stability. A similar technique was used to prepare the cladding substrate of our device (the lower level in Fig. 1), a borosilicate glass with similar thermal properties to SGBN (an important prerequisite when annealing direct-bonded samples at high temperatures<sup>4</sup>) and the high potassium content necessary to act as a source for  $\text{K}^+\text{-Na}^+$  ion-exchange<sup>3</sup>. Based on the chemical composition of commercially available BK-7<sup>10</sup>, our oxide mix was altered to allow an additional 4 wt.% (approx.) of  $\text{K}_2\text{O}$  into the glass by removing an equal amount of  $\text{Na}_2\text{O}$ , a composition previously used in the realisation of buried laser waveguides by intersubstrate ion-exchange<sup>9</sup>.

From each glass type a 2-mm-thick substrate, of 30 mm × 10 mm surface area, was diced and polished to provide an optically flat surface suitable for direct bonding. After cleaning, a mixture of  $\text{H}_2\text{O}_2\text{-NH}_4\text{OH-H}_2\text{O}$  (1:1:6), followed by several minutes of rinsing in deionised water, was applied to both materials in order to render their surfaces hydrophilic<sup>4</sup>. The doped and undoped layers were then brought into contact at room temperature and finger pressure applied in order to promote adhesive avalanche<sup>11</sup> between the two substrates, forcing out any excess air or liquid. Annealing of the sample at 350 °C for 6 hours provided ample bond strength for further machining and sufficient ion-exchange to create a single-mode planar waveguide layer on the photosensitive side of the bonded interface. The rare-earth doped side of the sample was then polished down to 200- $\mu\text{m}$ -thickness, and the end-faces of the device were diced and polished to a parallel optical finish.

Direct UV writing into the buried waveguide layer was performed using a frequency doubled argon laser at 244 nm

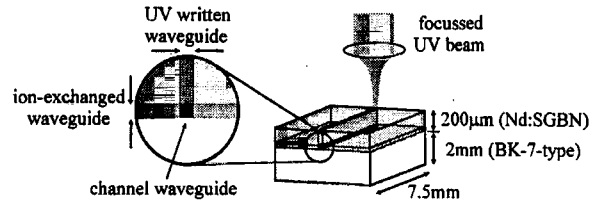


FIG. 2: Schematic diagram of a buried channel waveguide laser.

and high precision three-dimensional translation stage. A 35 mm lens was used to focus the UV beam to a 3.3- $\mu\text{m}$ -spot on the top surface of the sample, the beam waist of which was adjusted to coincide with the ion-exchanged layer for maximum intensity UV writing in this area. Channel confinement was created in the buried waveguide layer by translating the sample under the focussed UV beam, inducing a localised positive refractive index change in the photosensitive material<sup>5</sup>. The mechanism behind this effect has yet to be investigated but is likely to be similar to that observed in germanosilica-based optical fibers as the UV writing wavelength of 244 nm corresponds to the absorption peak for  $\text{GeO} \rightarrow \text{Ge}'$  defect formation (and subsequent refractive index change due to changes in material density) in such glass types<sup>12</sup>.

Optimisation of the channel waveguide geometry was performed by adjusting the writing intensity and translation speed of the focussed UV beam. Using a range of input powers of between 50 mW and 250 mW, and translation speeds of between 1  $\text{mm min}^{-1}$  and 10  $\text{mm min}^{-1}$ , it was determined that writing conditions of 200 mW input power with a translation speed of 10  $\text{mm min}^{-1}$  were suitable to give single-mode channel waveguide confinement in the buried ion-exchanged layer. Under these conditions over 80 single-mode channel waveguides were written into several similar devices, proving that this is a robust technology. A schematic diagram representing the dimensions of a typical buried channel laser waveguide device are given in Fig. 2.

Characterisation of laser performance and propagation loss of the device was performed with a tunable (700 nm to 850 nm) Ti-Sapphire laser using the typical arrangement illustrated in Fig. 3. Pump radiation was focussed for launch into each buried channel waveguide by means of a ×10 microscope objective with a measured input spot size of approximately 3  $\mu\text{m}$ . Optimisation of the launch was performed in relation to the fluorescence measured by a silicon detector, and an absorption of 31 % and launch efficiency of 13 % were calculated from measurements of input and output pump power from the waveguide. Laser action was achieved in the  $\text{Nd}^{3+} {}^4\text{F}_{3/2} \rightarrow {}^4\text{I}_{11/2}$  transition by butting plane mirrors to the end faces of the device and pumping a selected channel waveguide at 808 nm. Thresholds as low as 2.7 mW of absorbed power were obtained with these devices using two HR mirrors. With a 3 % output coupler the lasing threshold rose to 4.5 mW absorbed power and a slope efficiency of 9 % was obtained. Maximum output power with this configuration was 2 mW ( $\lambda = 1059 \text{ nm}$ ) for an absorbed power of 32 mW, although no effort was made to optimise the overlap of the pump and signal radiations (or neodymium content of the glass) for this initial demonstration.

Mode profiling of the output from the buried waveguide

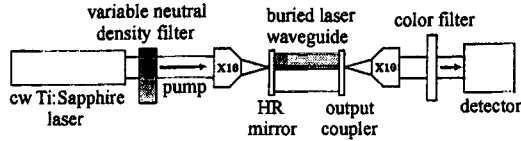


FIG. 3: Experimental arrangement for laser characterisation of the buried channel waveguide device.

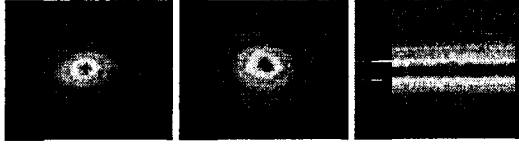


FIG. 4: Mode profiles for a) the pump and b) the laser transmission of a buried channel waveguide, and c) the pump transmission of the intersubstrate ion-exchanged buried planar waveguide layer.

was performed with a silicon camera and PC based evaluation software. It was observed that both the laser output and pump throughput were in the fundamental spatial-mode, with Gaussian mode profiles in both guided directions. A guided output spot size ( $1/e^2$  intensity radius) of  $3.4 \mu\text{m} \times 5.4 \mu\text{m}$  was measured for the laser output in the ion-exchanged and UV-written planes respectively, while the pump throughput spot size was  $2.9 \mu\text{m} \times 4.0 \mu\text{m}$ . Examples of typical mode profiles are presented in Fig. 4.

Propagation loss in the channel waveguide was estimated by investigating the relationship between laser threshold and output coupling<sup>13</sup>. Assuming negligible lower laser level population, constant loss with variable pump intensity, and constant laser mode size, the threshold of the laser,  $P_{th}$ , is expected to obey the equation:

$$P_{th} = k [2\alpha l - \ln(R_1 R_2)]$$

where  $k$  is a constant encompassing the pump and laser mode spatial properties and material parameters,  $l$  is the length of the monolithic cavity,  $R_1$  and  $R_2$  are the mirror reflectivities and  $\alpha$  is the propagation loss coefficient. By varying the output coupler a plot of threshold against  $-\ln(R_1 R_2)$  was produced (Fig. 5), the x-axis intercept of which gives an estimate of propagation loss. For our buried channel waveguides a value of  $2.3 \text{ m}^{-1}$  was measured for  $\alpha$ , corresponding to a loss of  $0.1 \text{ dB cm}^{-1}$ . While the availability of suitable mirror sets limited these results to just three points on the graph, this result was confirmed with a separate calculation of the expected slope efficiency<sup>14</sup> (using the measured spot sizes and an assumed quantum efficiency of 100 %) giving an upper limit for propagation loss of  $0.3 \text{ dB cm}^{-1}$ . This is comparable to the losses achieved in direct-UV-written germanosilica-based wafers<sup>5</sup> and to those achieved by alternative  $\text{K}^+\text{-Na}^+$  ion-exchange processes in neodymium-doped borosilicate glass<sup>2</sup>.

In conclusion, we have reported a fabrication technique for the production of low-loss single-mode buried laser channel waveguides in neodymium-doped SGBN glass. The key to this process is the combination of direct bonding, which provides a buried waveguide layer in the photosensitive glass by intersubstrate ion-exchange, and direct UV writing, which is used to create channel waveguide confinement in that layer. Characterisation of laser performance in the buried channel waveguides demonstrates milliwatt-order laser thresholds, single-spatial-mode

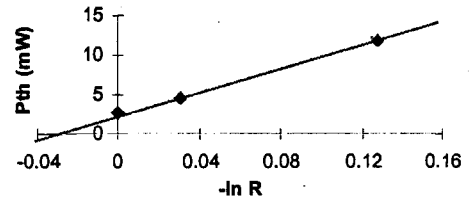


FIG. 5: Dependence of laser threshold power with output coupling.

operation, and propagation losses of  $< 0.3 \text{ dB cm}^{-1}$ . These initial results suggest that optimisation of glass composition and UV writing conditions could lead to efficient low-loss buried channel waveguide devices and UV-written structures for use with integrated optics. The potential for bonding large wafers of material (to be diced into many smaller devices) for the mass production of complex UV-written devices could also prove ideal for fabricating laser waveguides with long absorption lengths, such as erbium-doped devices. More generally, the combination of direct bonding and direct UV writing provides extra degrees of design freedom in the realisation of 2D and 3D integrated waveguide structures in multicomponent photosensitive glass.

The Optoelectronics Research Centre is an interdisciplinary research centre supported by the Engineering and Physical Sciences Research Council (EPSRC). Work performed at the Politecnico de Torino was partly supported by the Italian Research Council (CNR) under the finalized project MADESS-II and by Pirelli Optical Components.

- [1] R. V. Ramaswamy and R. Srivastava, *J. Lightwave Tech.* **6**, 984 (1988).
- [2] E. Mwarania, J. Wang, J. Lane, and J. S. Wilkinson, *J. Lightwave Tech.* **11**, 1150 (1993).
- [3] C. B. E. Gawith, T. Bhutta, D. P. Shepherd, P. Hua, J. Wang, G. W. Ross, and P. G. R. Smith, *Appl. Phys. Lett.* **75**, 3757 (1999).
- [4] J. Haisma, B. A. C. M. Spierings, U. K. P. Biermann, and A. A. van Gorkum, *Appl. Opt.* **33**, 1154 (1994).
- [5] M. Svalgaard, C. V. Poulsen, A. Bjarklev, and O. Poulsen, *Elec. Lett.* **30**, 1401 (1994).
- [6] M. Svalgaard, *ECIO*, 333 (1999).
- [7] M. Svalgaard, *Elec. Lett.* **33**, 1694 (1997).
- [8] D. Milanese, A. Fu, C. Contardi, E. R. M. Taylor, and M. Ferraris, *Opt. Matls.* **18**, 295 (2001).
- [9] G. Perrone, A. Moro, C. Contardi, and D. Milanese, *Elec. Lett.* **36**, 1845 (2000).
- [10] C. Ciminelli, A. D'Orazio, M. De Sario, C. Geradi, V. Petruzelli, and F. Prudeniano, *Appl. Opt.* **37**, 2346 (1998).
- [11] J. Haisma, G. A. C. M. Spierings, T. M. Michielsen, and C. L. Adema, *Philips J. Res.* **49**, 23 (1995).
- [12] R. Kashyap, *Fiber Bragg gratings*, Academic Press (1999).
- [13] D. Findlay and R. A. Clay, *Phys. Lett.* **20**, 277 (1966).
- [14] W. P. Risk, *J. Opt. Soc. Amer. B*, **5**, 1412 (1988).